Cytometry 8:445–452 (1987)

Multiple Wavelength Illumination in Flow Cytometry Using a Single Arc Lamp and a Dispersing Element

B.G. de Grooth, M. van Dam, N.C. Swart, A. Willemsen, and J. Greve
Department of Applied Physics, Twente University of Technology, 7500 AE Enschede, The Netherlands

Received for publication November 27, 1985; accepted January 26, 1987

The principle of a multiple wavelength illumination method for flow cytometers, based upon a combination of a helium-neon laser and an arc lamp as illumination sources is described. By using a prism, the light from the arc lamp is dispersed and the different colors are imaged at different places on the sample stream. The small angle light scattering from the helium-neon laser light is measured as a relevant parameter and serves as a trigger signal for subsequent measurements of fluorescence or scattering of light from the arc lamp. Two experimental systems are described utilizing this principle: a system where the emission is detected orthogonally with respect to the direction of the illumination beams, and an epi-illumination system.

With the orthogonal set-up multiple wavelength right angle scattering measurements are possible. This is illustrated by showing that the orthogonal scattering from erythrocytes is strongly dependent on the illumination wavelength. It is further shown that the apparatus is suitable for the measurement of intracellular pH using the pH dependence of the excitation spectrum of fluorescein.

The epi-illumination system allows excitation of two (or more) fluorescent dyes with different excitation spectra. In this case the emission spectra of the fluorescent dyes may overlap substantially. This is shown by simultaneous measurement of DNA and protein of Chinese hamster lung cells using mitramycin and tetramethyl rhodamin isothiocyanate (TRITC).

Key terms: Intracellular pH measurement, DNA-protein staining, prism

Multiple wavelength illumination significantly increases the possibilities of flow cytometers. For an extensive and comprehensive article on the applications of multiple wavelength illumination the reader is referred to the review of Shapiro (12). The necessary apparatus can be built relatively easily by adding one (1,5,16,19) or two (11,17) lasers to an existing laser based flow cytometer. However, the high purchase and maintenance costs of the lasers make this solution impractible for most users. As an alternative to the laser systems, incoherent light sources such as xenon and mercury arc lamps can be used. For example, the original multistation flow cytometer of Curbelo et al.(4) was equipped with a high pressure xenon arc lamp. The successful use of conventional lamps as inexpensive light sources for flow cytometry, both in laboratory (8,10,14,15,21) and in commercial systems (Phywe ICP, Leitz MPV, Becton Dickinson FACS Analyser), has led us to reexamine the use of these lamps for multiple wavelength illumination flow cytometers. Here we describe a flow cytometer that utilizes a single arc lamp and a dispersing prism to achieve multiple wavelength illumination. In order to get a strong and reliable signal that is dependent on cell size, and to obtain an unambiguous trigger signal, we have included a helium-neon laser in the system.

MATERIALS AND METHODS

The measurements described here were done with a home-made flow cytometer, developed for flexible use in different experimental configurations. The flow chamber is built from the rectangular quartz capillary of Precision Cells (Hicksville, NY). The pressure of the flow system was regulated with Fairchild regulators (model 15).

A 100-W mercury arc lamp (HBO 100 Osram) mounted in a Leitz lamphouse and a 5-mW helium-neon laser (Spectra Physics Model 120) were used as light sources. Small-angle light scattering from the laser was detected with a photodiode (PIN 10 D, United Detector Technology); orthogonal light scattering and fluorescence measurements were done with a photomultiplier with S20 (EMI, 9659 B) or multialkali (Hamamatsu, R 928) cathode.

Address reprint requests to B.G. de Grooth, Twente University of Technology, Department of Applied Physics, P.O. Box 217, 7500 AE Enschede, The Netherlands.

Mechanically, the system is built up from modular units that can be mounted on a bottom frame. The detector signals are analyzed with a home-made 2-parameter multichannel analyzer. The system consists of amplifiers, peak detectors, sample and hold circuits, two ADCs (12 bits successive approximation, Datel model EH 12 B3), and a 128 × 128 × 16-bit memory. Data are stored as two-dimensional histograms with a resolution of 128 channels for each parameter. A connection with an LSI 11/23 minicomputer allows the user to view the results during measurements on a graphic display, store the data on floppy disks for further analysis, and plot the results with a HP7470-A (Hewlett Packard) plotter. Two-parameter measurements of sequentially occurring signals are done with an electronic processing circuit similar to that described by Steinkamp and Hiebert (18).

Peripheral human blood cells were obtained from healthy donors using sodium heparine as the anticoagulant. Lysis of erythrocytes was done by incubating a pellet of blood cells for 10 minutes at room temperature with 155 mM NH_4Cl, 10 mM $KHCO_3$, and 0.1 mM EDTA. After lysing, the cells are washed twice with phosphate buffered saline (PBS).

Chinese hamster lung cells (CHL-cells) were cultured in the laboratory in minimal essential medium. DNA staining with Mithramycin (100 μg/ml) was done according to the method outlined by Chrissman and Tobey (2) Protein staining with tetramethyl rhodamin isothiocyanate (TRITC) (30 μg/ml) was done as described by Cornelisse and Ploem (3). Calibration of the pH dependence of infracellular fluorescein fluorescence was done with CHL cells washed twice in phosphate/citric acid buffer containing 250 mM KCL. Appropriate amounts of 100 mM Na_2PO_4 and 60 mM citric acid were mixed to obtain pH values of 6.5 and 7.5; 15 minutes prior to the measurements the cells were incubated with 0.3 mM fluorescein diacetate (FOA). Nigericin (5.5 μM), valinomycin (3 μM), and gramicidin (3μM) were added in order to equilibrate the internal pH of the cells with the pH of the external buffers. Excitation spectra of fluorescein (final concentration 0.3 μg × ml^{-1}) emitted above 520 nm at different pH were measured with a Perkin-Elmer LS-3 spectrophotometer. The pH of the fluorescein solvent was obtained by appropriate mixture of the phosphate and citric acid buffers described above.

Monodispersed latex particles (4.7 and 2.9 μm diameter with standard deviations of less than 2%) were purchased from Polysciences Inc. (Warrington, PA).

RESULTS

Description of the Illumination System

The principle used here for multiple wavelength illumination is illustrated in Figure 1. The arrangement consists of a conventional Köhler illumination system equipped with a dispersing element placed in front of the illumination objective. Since a high resolution was not required we have used a simple prism as the dispersing component in this study, although in principle a grating can be used as well. With this optical arrangement the different wavelengths emitted by the arc lamp are imaged at different places on the particle stream in the flow chamber. The spectral purity of these images is inversely proportional to the diameter of the image diaphragm at the collector lens and proportional to the dispersion of the prism. The spatial distance between spots of different wavelength is determined by the focal length of the illumination lens and the dispersion of the prism. The intensity at the sample stream is proportional to the square of the numerical aperture of the illumination objective. The measured signal is proportional to the time the object is illuminated and therefore proportional to the diameter of the condensor diaphragm. Table 1 shows the positions of the dominant spectral lines of a 100-W mercury arc lamp in the flow chamber calculated for two prisms (Flint-F2 and Crown BK7, Melles Griot) and two different lens systems used for illumination (Leitz H32× objective, numerical aperture 0.6, focal length 8 mm, and a Wild condensor model 6070, numerical aperture 0.9, focal length 14 mm). In this study we have chosen the Leitz H32 objective and F2 prism. For the practical realization of a complete flow cytometer using this illumination method, we have added a helium-neon laser to the system. Just before a cell is illuminated by the spectrum of the arc lamp, the cell crosses the beam of the helium-neon laser. This was done for two reasons. Firstly, the resulting light scattering pulses serve as a trigger signal for the subsequent measurements so that it is known in principle from the time delay with respect to the trigger signal from which excitation wavelength a measured signal originates. Secondly, the forward light scattering, the orthogonal

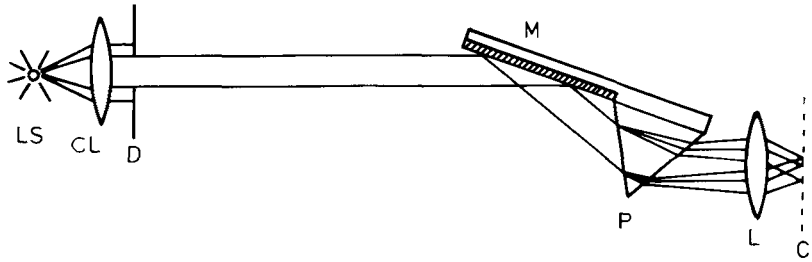

FIG. 1. Schematic illustration of the principle used to obtain multiwavelength illumination for arc lamp based flow cytometers. Due to the dispersion of the prism, the different spectral lines of the arc lamp are imaged at different positions on the particle stream. In our experimental set-up the diaphragm (D) is imaged at the sample stream (Köhler illumination, not shown in detail). LS, light source; CL, condensor lens; L, illumination lens; D, diaphragm; M, mirror; P, prism; C, cellstream.

Table 1
Positions on the Sample Stream of the Most Intense Lines of a 100-W Mercury Arc Lamp[a]

Wavelength (nm)	Leitz H32 objective		Wild condensor	
	BK7 prism position (μm)	F_2 prism position (μm)	BK7 prism position (μm)	F_2 prism position (μm)
365	0	0	0	0
405	75	228	132	400
436	119	350	209	614
546	217	497	381	1,045
577	237	542	415	1,124

[a]Calculated for two illumination lenses and two types of prism materials. The position of the 365-nm line was arbitrarily chosen as origin.

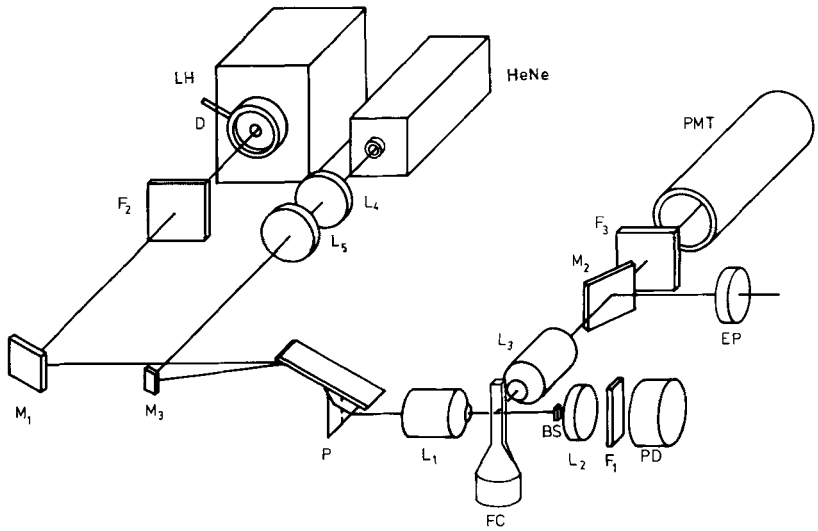

FIG. 2. Schematic drawings of the orthogonal set-up employing the principle outlined in Figure 1. LH, lamphouse; HeNe, helium-neon laser; m_1-m_3, mirrors; P, prism; L_1-L_5, lenses; FC, flowcell; BS, beam stop; D, diaphragm; F_1-F_3, filters; PD, photodiode; PMT, photomultiplier; EP, eyepiece.

light scattering, and the fluorescence caused by the helium-neon laser can be measured as relevant parameters as well.

We have done experiments with two configurations. In the first setup (Fig. 2), illumination by the arc lamp and the helium-neon laser is achieved by a single objective lens (Leitz H 32×, numerical aperture 0.6) whereas the emitted fluorescence and orthogonal scattering is detected via a second objective (Leitz L 32×, numerical aperture 0.4) mounted perpendicular to the first one. In the second setup, shown in Figure 3, fluorescence is measured with an epi-illumination system while the helium-neon laser beam is directed orthogonally to the axis of the epi-illumination system. This configuration allows measurement of the light scattering originating from the helium-neon laser. The proper beam diameter of the laser waist at the intersection point with the particle stream required for a homogeneous illumination intensity over the width of the core stream can be obtained by selecting a lens with an appropriate focal length. We have used a lens L_1 with a focal length of 80 mm, which yields a waist of about 80 μm ($1/e^2$ points) (13).

Measurements with the helium-neon laser are more difficult to realize in the setup shown in Figure 2, since here the laser beam is focused by the same objective as is used for the arc lamp illumination. In order to obtain a high intensity of the arc lamp light on the sample core, a high numerical aperture is required, which means in practice a relative short focal length. For the objective used, the focal length is 8 mm. If the virtually parallel light beam emitted by the helium neon laser is focussed directly by this objective on the sample stream, the spot size would be 8 μm (13). This is of course too small for a homogeneous illumination of the cells in the sample core required for significant measurements.

This problem was solved by inserting two lenses in the laser beam optics (see Fig. 2, lenses L4 and L5). With these lenses the laser beam is first focused in the back-focus of the illumination objective. Thus, a virtually parallel light beam is obtained between the illumination objective and the beam stop. We have used focal lengths of 10 mm and 30 mm for L4 and L5 respectively. With the Leitz H32 illumination objective placed at an optical distance of 42 cm from L5, we obtain a parallel laser beam of 50 μm ($1/e^2$ points) at the sample stream. In

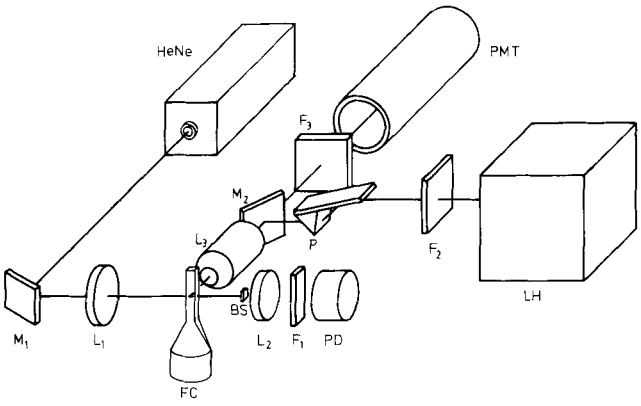

FIG. 3. Schematic drawings of the multiwavelength epi-illumination flow cytometer. Symbols defined as in Figure 2.

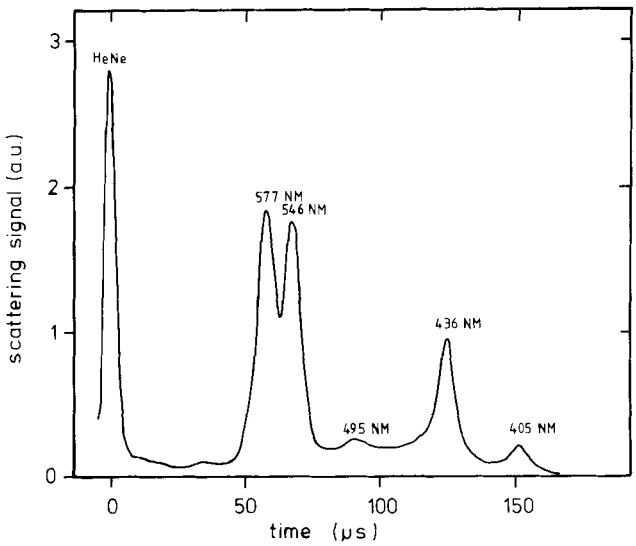

FIG. 4. Time dependence of the orthogonal light scattering of a 4.7-μm latex particle measured with the set-up of Figure 2 using a digital storage scope. The first peak represents the scattering of the helium-neon laser, the relative amplitude of which was suppressed by a short wavelength pass filter. The subsequent peaks are due to the spectral lines of the mercury arc lamp.

order to get the laser spot at the right position on the sample stream, the direction of the incident laser beam must be different from that of the arc lamp light beam, as a consequence of the dispersion of the prism. Thus, the simultaneous illumination of both light sources can be achieved without light losses caused by a beam splitter or a dichroic mirror (see Fig. 2). The diaphragm (D) in front of the condensor lens, which is imaged on the particle stream, can be translated in two directions. The helium-neon laser beam is directed to the prism via a mirror (M_3, Fig. 2), which can be rotated and translated. In this way the laser light and the mercury arc lamp light can be adjusted independently on the sample stream. By viewing through the eyepiece, the interior of the flow cell can be seen and the adjustment of the light beams on the particle stream is very simple.

Experimental Results

Figure 4 shows the time dependence of the orthogonal light scattering signal of a single polystyrene sphere (4.7 μm diameter), obtained with the system outlined in Figure 2. The first relatively sharp peak is due to the light scattering from the helium-neon laser. The subsequent peaks are due to orthogonal light scattering of the 577-, 546-, 495-, 436-, and 405-nm spectral lines of the mercury arc lamp, respectively. It should be noticed that in the figure the relative intensity of the helium-neon laser peak in comparison to the arc lamp lines was greatly reduced by using a 600-nm short wavelength pass filter in the detection optics (F_3 in Fig. 2). Light scattering from the ultraviolet line at 365 nm was not observed since the objectives used had a poor transmission in this spectral region. The helium neon laser illumination method applied in the orthogonal set-up yields satisfactory results. With polystyrene spheres with a diameter of 2.9 μm we routinely obtain histograms of the forward light scattering signal with a coefficient of variation (CV) of less than 4%. Figure 5 shows a density map of the forward versus orthogonal light scattering obtained with normal human blood cells after lysing most of the erythrocytes. The familiar pattern is visible with clusters due to granulocytes, monocytes, lymphocytes, and unlysed erythrocytes, thrombocytes, and cell debris. For the leucocytes, virtually identical plots were obtained when the small angle helium-neon light scattering was plotted versus the orthogonal light scattering of the 577-, 546-, 436-, or 405-nm light from the mercury arc lamp. However, the relative intensity of the light scattered orthogonally by erythrocytes was much smaller at 405 and 436 nm. This is clearly shown in Figure 6, where the right angle light scattering was measured simultaneously at 405 and 577 nm. The granulocytes, monocytes, and lymphocytes appear in the density map on a single straight line, but the erythrocytes are located on a different line. The apparent deviation from linearity near the origin is due to a small nonlinearity in the electronic circuit. For red blood cells, the ratio of the orthogonal light scattering measured at 405 and 577 nm is almost 4 times smaller than for leucocytes.

An interesting application for multiple wavelength flow cytometry is the measurement of intracellular pH employing the pH dependence of the excitation spectrum of fluorescein. The method has been used in a number of laboratories using quantitative microscopy (6,7,20) and has been suggested for flow cytometry by Visser and Tanke (22). These authors could not test the method since the two lasers required for the measurement were not available. The mercury arc lamp is well suited for these experiments using the spectral lines at 495 and 436 nm as excitation wavelengths. The ratio of the emitted fluorescence intensities of fluorescein excited at these wavelengths is strongly pH dependent (Fig. 7), in agreement with Jamieson et al. (7). We have loaded CHL cells intracellular with fluorescein by addition of FDA. The intracellular pH was equilibrated with

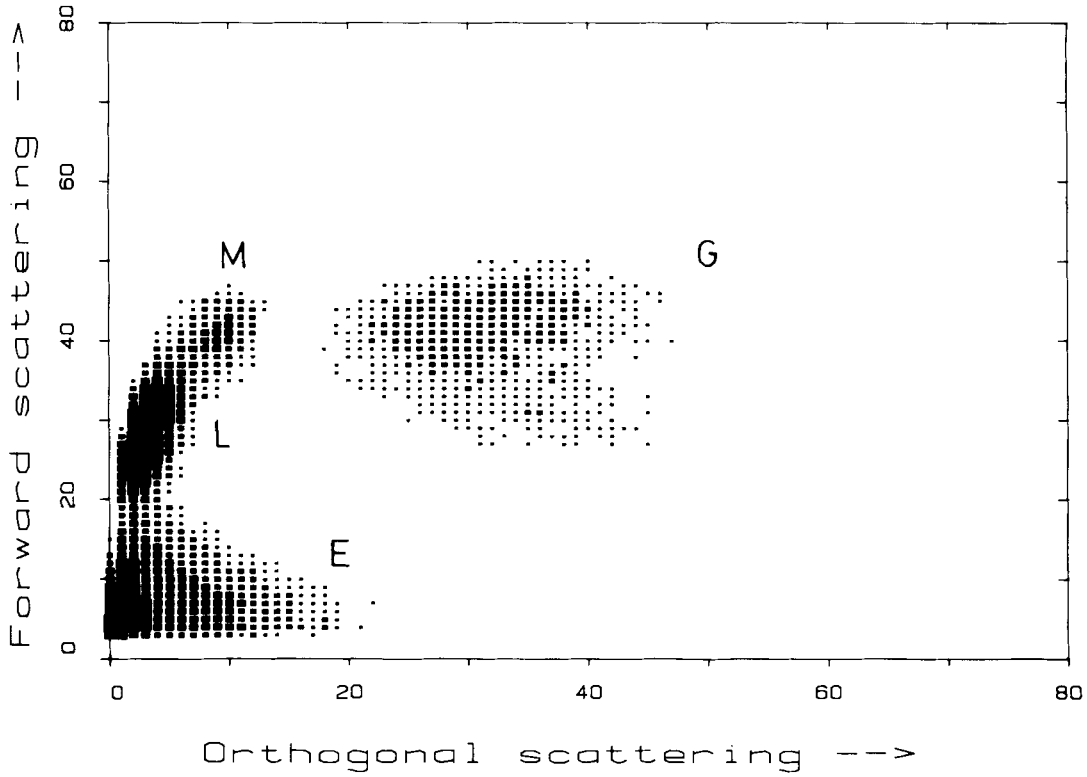

FIG. 5. Density map of forward and right angle light scattering of lysed human blood cells. The figure was obtained with the helium-neon laser using the optical arrangement of Figure 2. Clusters due to granulocytes (G), monocytes (M), lymphocytes (L), and erythrocytes with cell debris (E) are clearly resolved.

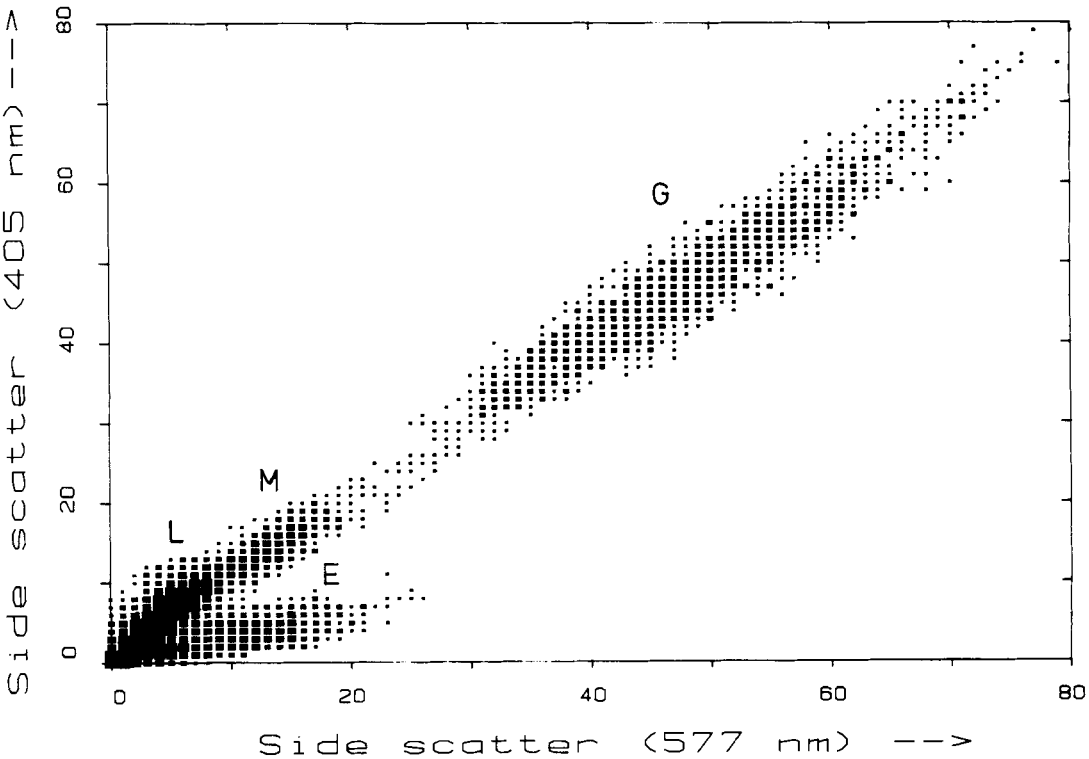

FIG. 6. Density map of orthogonal light scattering of lysed human blood cells measured simultaneously at 405 and 577 nm. The granulocytes (G), monocytes (M), and lymphocytes (L) appear on a single straight line. The erythrocytes (E) show a relatively low scattering at 405 nm.

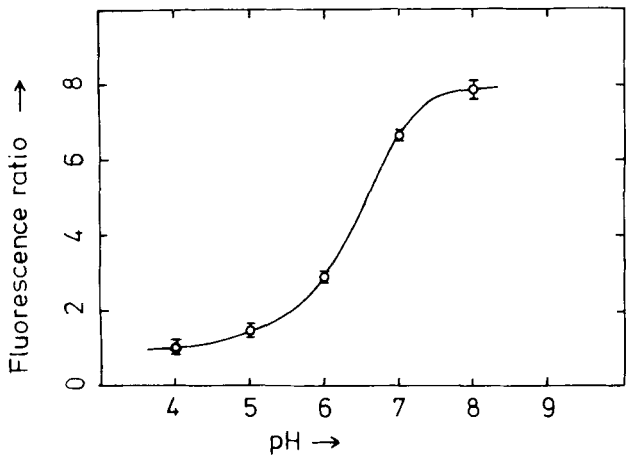

FIG. 7. pH dependence of the ratio of fluorescein fluorescence excited at 495 and 436 nm measured in a spectrophotometer. The pH was adjusted by a mixture of citric acid and phosphate buffers (see Materials and Methods).

the extracellular pH by addition of ionophores valinomycin, nigericin, and gramicidin. The apparatus outlined in Figure 2 was equipped with a 500-nm short pass excitation filter (F_2) and a 515-nm long pass filter (F_3). The fluorescence intensities excited at 436 and 495 nm were measured simultaneously both at an external pH of 6.5 and at an external pH of 7.5. The results of these two experiments are plotted in the density map of Figure 8. The figure reveals four populations due to vital and dead cells at both pH values. The ratio of the fluorescence intensities excited at 495 and 436 nm increased 1.45–1.55 times when the pH was raised from 6.5 to 7.5. This is in good agreement with the value of 1.55 that can be obtained from Figure 7 for free fluorescein.

Multiple wavelength excitation with the epi-illumination apparatus of Figure 3 is illustrated with simultaneous DNA and protein staining applied to CHL cells. We have chosen mithramycin as a DNA stain (2) and TRITC as a protein stain (3). The combination of these dyes is well suited for the purpose of demonstrating the multiple wavelength excitation principle, since their excitation spectra are different whereas their emission spectra largely overlap (12). Mithramycin was excited by the 405- and 436-nm mercury lines whereas TRITC was excited by the 546-nm line. Fluorescence of both fluorochromes was detected with the same photomultiplier provided with 590-nm longwavelength pass filter. The results are shown in Figure 9.

DISCUSSION

We have shown here that multiple wavelength illumination in flow cytometry can be obtained with a relatively simple optical system consisting of a helium-neon laser and an arc lamp. The spectral resolution obtained with the prism system can be estimated from the orthogonal scattering experiment of microspheres shown in Figure 4. In this experiment the resolution is about 8 nm in the violet region of the spectrum and about 20 nm

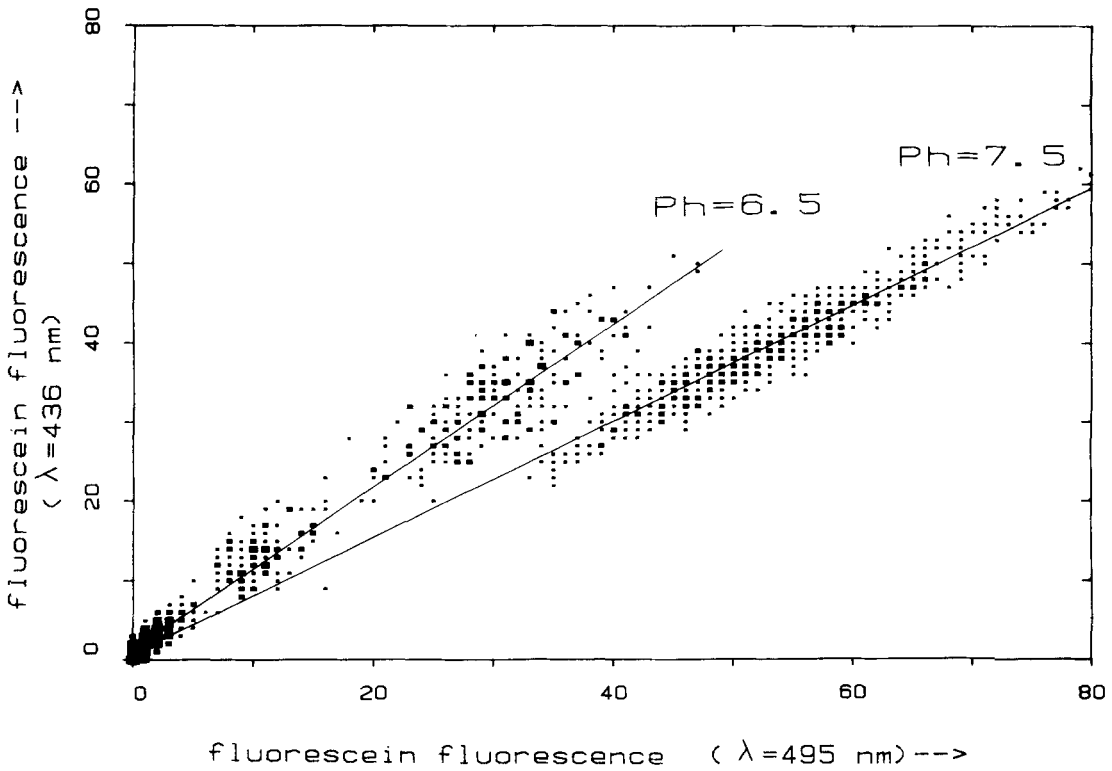

FIG. 8. Flow cytometric density map of fluorescent CHL-cells excited at 495 and 436 nm. The cells are incubated with FDA and equilibrated with an external pH of 6.5 and 7.5 in two separate experiments.

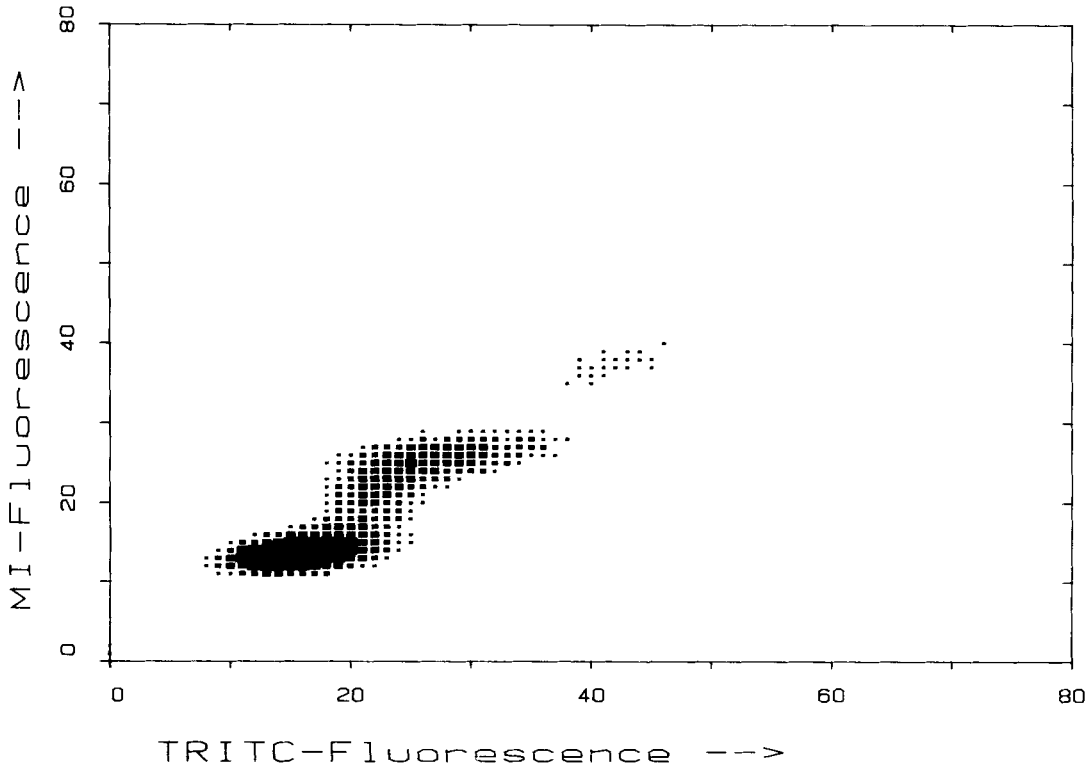

FIG. 9. Flow cytometric density map of a sample of CHL-cells, stained with mithramycin (MI—DNA content) excited at 436 nm and TRITC (protein content) excited at 546 nm. The epi-illumination system of Figure 3 was used with: F_2, BG38 (Shott) + short wavelength pass 550 nm (Melles Griot); F_3 KV550 and OG590 (Shott) M_2, long wavelength pass 650 nm (Melles Griot). M_2 is placed at an angle of 45° with respect to the incident light; therefore the wavelength of 50% transmission is shifted to about 600 nm.

around 577 nm. In principle this resolution can be improved by diminishing the size of the condensor diaphragm or by choosing a prism with a larger dispersion. However, for most applications the spectral resolution obtained here is more than sufficient. The use of the helium-neon laser gives a strong forward light scattering signal that provides a reliable trigger signal, which in addition can be used for measurement of forward and orthogonal light scattering. We have experimented with two optical configurations, outlined in Figures 2 and 3. Both systems have advantages and disadvantages. The main advantage of the epi-illumination system is that it allows the use of objectives with high numerical apertures, so that weak fluorescing objects can be measured efficiently. In the orthogonal system, the obvious geometrical restrictions limit the numerical aperture of the objectives to about 0.6. The orthogonal system has the advantage that the illumination and detection optics are completely separated. This makes it possible to measure dual wavelength excitation fluorescence in those cases where a strong spectral overlap exists between the emission spectrum of one fluorochrome and the excitation spectrum of a second fluorochrome. In practice this is impossible with an epi-illumination system. Here the objective and beam splitter (L3 and M_2 of Fig 3) are illuminated directly by the excitation light. The inevitable scattering and reflections of these components cause an intolerable amount of background light.

As was outlined in Results, a principle difficulty arises when arc lamp and laser illumination are combined with a single illumination objective. We have shown that the addition of L4 and L5 in the orthogonal set-up of Figure 2 indeed solved this problem; the observed CV of less than 4% indicates that the laser illumination is sufficiently homogenous over the sample stream.

Our results with multi-color orthogonal light scattering show that within the experimental accuracy, all leucocytes have the same wavelength dependence for this type of scattering between 405 and 630 nm. The erythrocytes show a relative low side scattering at 405 and 436 nm. This is presumably due to the high absorption of the erythrocytes in this spectral region.

The multiple wavelength illumination method can be used for measurement of intracellular pH (Fig. 8). From the slope of Figure 7 and the accuracy by which the fluorescence excitation ratio can be determined (Figure 8), it can be estimated that around pH 6.5 intracellular pH changes of 0.2 pH units of a cell population are detectable. Murphy et al.(9) have described an alternative method for the determination of intracellular pH with a flow cytometer using a single argon laser. In their method the cells are loaded with two different dyes, one (FITC) with pH dependent fluorescence, the other (TRITC) pH independent. This method, however, is based on the assumption that both dyes are bound to exactly the same components. It would be interesting to

compare both methods in order to test whether this condition is fulfilled or not for different cells.

As an example of the epi-illumination system we have shown a simultaneous DNA-protein measurement using mitramycin and TRITC. Although this can be done much more easily with a single wavelength illumination, using, e.g., FITC (protein) and propidium iodide (DNA) (2), we have chosen this experiment to illustrate the possibilities of the apparatus.

The emission spectra of mitramycin and TRITC strongly overlap so that a multiple wavelength illumination is necessary for a simultaneous measurement of these dyes. The results show that independent measurement of both dyes is indeed possible, even with a single photomultiplier.

It should be noted, however, that selectively imaging the illumination stations on separate photomultipliers is to be preferred; first of all, optimal filters for the different dyes can be placed in front of the detectors, and secondly, artificial signals caused by cells passing during the dead time of the electronic system are eliminated in this way.

ACKNOWLEDGMENTS

We thank C.J. van Doorn, A. Florians, and G.M.J. Segers-Nolten for skillful mechanical, electronic, and analytical work, respectively.

LITERATURE CITED

1. Arndt-Jovin DJ, Grimwade BG, Jovin TM: A dual laser flow sorter utilizing a CW pumped dye laser. Cytometry 1:127–131, 1980.
2. Chrissman HA, Tobey RA: Cell cycle analysis in 20 minutes. Science 184:1297–1298, 1974.
3. Cornelisse CJ, Ploem JS: A new type of two-color fluorescence staining for cytology specimens. J Histochem Cytochem 24:72–81, 1976.
4. Curbelo R, Schildkrant ER, Hirschfeld T, Webb RH, Block MJ, Shapiro HM: A generalized machine for automated flow cytology system design. J Histochem Cytochem 24:388–395, 1976.
5. Dean PN, Pinkel D: High resolution dual laser flow cytometry. J Histochem Cytochem 26:622–627, 1978.
6. Heiple JM, Taylor DL: Intracellular pH in single motile cells. J Cell Biol 86:885–890, 1980.
7. Jamieson GA, Frazier WA, Schlesinger PH: Transient increase in intracellular pH during Dictyotelium differentiation. J Cell Biol 99:1883–1887, 1984.
8. Lindmo T, Steen HB: Characterisation of a simple, high resolution flow cytometer based on a new flow configuration. Biophys J 28:33–44, 1979.
9. Murphy RF, Powers S, Cantor CR: Endosomal pH measurement in single cells by dual fluorescence flow cytometry: Rapid acidification of insulin to pH 6. J Cell Biol 98:1757–1762, 1984.
10. Olson RJ, Frenkel SL, Chisholm SW, Shapiro HM: An inexpensive flow cytometry for the analysis of fluorescent signals in phytoplankton: Chlorophyll and DNA distributions. J Exp Mar Biol Ecol 68:129–144, 1983.
11. Shapiro HM, Schildkraut R, Curbulo R, Brough-Turner R, Webb R, Brown P, Block MJ: Cytomar R: A computer controlled multiple laser source multiparameter flow cytophotometer system. J Histochem Cytochem 25:836–844, 1977.
12. Shapiro HM: Multistation multiparameter flow cytometry: A critical review and rationale. Cytometry 3:227–243, 1983.
13. Shapiro HM: Practical Flow Cytometry. Alan R. Liss. Inc., New York, 1985, p 42.
14. Steen HB, Lindmo T: Flow cytometry: A high resolution instrument for everyone. Science 204:403–404, 1979.
15. Steen HB: Further developments of a microscope based flow cytometer: Light scatter detection and excitation intensity compensation. Cytometry 2:26–31, 1980.
16. Steinkamp JA, Orlicky DA, Crissman HA: Dual-laser flow cytometry of single mammalian cells. J Histochem Cytochem 27:273–276, 1979.
17. Steinkamp JA, Stewart CC, Crissman HA: Three-color fluorescence measurements on single cells excited at three laser wavelengths. Cytometry 2:226–231, 1982.
18. Steinkamp JA, Hiebert RD: Signal processing electronics for multiple electronic and optical measurements on cells. Cytometry 2:232–237, 1982.
19. Stöhr M, Eipel H, Goerttler K, Vogt-Schaden M: Extended application of flow microfluorometry by means of dual laser excitation. Histochemistry 51:305–313, 1977.
20. Thomas JA, Buchsbaum RN, Zimmiak A, Racker E: Intracellular pH measurement in Ehrlich ascites tumor cells utilizing spectroscopic probes generated in situ. Biochemistry 18:2210–2218, 1979.
21. Van Sengbusch G, Hugeman B: A fluorescence microscope attachment for flow-through cytofluorometry. Exp Cell Res 86:53–60, 1974.
22. Visser JWM, Jongeling AAM, Tanke HJ: Intracellular pH-determination by fluorescence measurements. J Histochem Cytochem 27:32–35, 1979.